ISSN: 2458-8989

Natural and Engineering Sciences

NESciences, 2026, 11 (3): 132-141 doi: 10.28978/nesciences.263012

Morphometric, Histopathological, and Immunohistochemical Evaluation of Myocardial Remodeling in Cisplatin-Induced Renal Failure in Rats

Kosimov Umid Usmonovich [1], Turniyozov Azamat Askarovich[2], Bakhronov Jurat Djurakulovich[3], Teshaev Ulugbek Shukhratovich[4], Khidirov Ziyadulla Erkinovich[5], Qodirov Oybek O‘ktam o‘g‘li [6]

[1]Doctor of the pediatric intensive care unit of the Bukhara branch of the Scientific Center for Emergency Medical Care of the Republic of Uzbekistan. ORCID: 0009-0000-1298-2329 E-mail: umedqosimov814@gmail.com

[2]Head of the Cardiology Department of the Republican Scientific Center for Emergency Medical Care of the Navoi Branch (Navoi, Republic of Uzbekistan). ORCID: https://orcid.org/0009-0007-5246-3698, E-mail: turniyozovazamat@gmail.com

[3]Doctor of Medical Sciences, Professor, Head of the Department of Histology, Cytology and Embryology of the Bukhara Medical Institute (Bukhara, Republic of Uzbekistan). ORCID: 0000 0002 9178 3367, E-mail: bahronovjurat7@gmail.com

[4]Assistant of the Department of Faculty and Hospital Surgery, PhD. Bukhara State Medical Institute named after Abu Ali ibn Sino. Bukhara, Uzbekistan. ORCID: https://orcid.org/0009-0000-0052-2827, E-mail: ulug_leo@mail.ru

[5]Human Anatomiya Assistant. Samarkand state medical University. Samarkand, Uzbekistan. ORCID: https://orcid.org/0009-0000-2681-9610, E-mail: xidirovziyadulla@gmail.com

[6]Department of Gistology, Sitology Va Embryology, Bukhara State Medical Institute named after Abu Ali ibn Sino, Bukhara, Republic of Uzbekistan. ORCID: https://orcid.org/0009-0000-1723-4303, E-mail: oybek_qodirov@bsmi.uz

Abstract

Experimental renal failure is associated with systemic pathological alterations affecting the cardiovascular system. This study aimed to evaluate morphometric, histopathological, and immunohistochemical changes in the myocardium of rats with cisplatin-induced renal failure.

Morphometric analysis revealed progressive myocardial remodeling characterized by increased thickness of the endocardium, myocardium, and epicardium, as well as enlargement of cardiomyocytes and expansion of myocardial stromal tissue. Histopathological examination demonstrated vascular congestion, endothelial swelling, luminal narrowing, interstitial edema, inflammatory cell infiltration, and degenerative changes in cardiomyocytes.

Immunohistochemical analysis showed positive p53 expression in 37.75% of myocardial cells, indicating activation of apoptosis-related pathways. The severity of structural alterations increased with age and was accompanied by progressive vascular and stromal remodeling.

These findings demonstrate that cisplatin-induced renal failure causes significant myocardial injury through mechanisms involving microcirculatory disturbances, inflammation, and apoptosis, providing morphological evidence for the development of cardiorenal syndrome.

Corresponding Author: Qodirov Oybek O‘ktam o‘g‘li, E-mail: oybek_qodirov@bsmi.uz

Keywords
Renal Failure, Myocardium, Morphometry, Cardiomyocytes, Cisplatin, Cardiorenal Syndrome, Histopathology, Experimental Rats.

Available online: 01/09/2026

Introduction

Recent studies have increasingly emphasized the close relationship between renal dysfunction and cardiovascular pathology. Renal failure is recognized as a systemic disorder that affects multiple organs and tissues, particularly the cardiovascular system, through complex hemodynamic, metabolic, and inflammatory mechanisms (Rangaswami et al., 2023).

Experimental and clinical investigations have demonstrated that progressive impairment of kidney function promotes the accumulation of uremic toxins, oxidative stress, endothelial dysfunction, and chronic inflammatory activation (House et al., 2022). These pathological processes contribute significantly to myocardial injury and accelerate the development of structural and functional cardiac abnormalities (Kooman et al., 2023).

Among available experimental models, cisplatin-induced nephrotoxicity remains one of the most widely used approaches for investigating renal injury and its systemic consequences. Cisplatin administration produces severe tubular epithelial damage accompanied by oxidative stress, inflammatory responses, and apoptosis (Pabla & Dong, 2022). These pathological mechanisms extend beyond the kidneys and contribute to secondary damage in distant organs, including the myocardium (Ozkok & Edelstein, 2023).

Recent evidence further indicates that cisplatin may exert direct cardiotoxic effects in addition to its nephrotoxic action, resulting in myocardial oxidative stress, endothelial dysfunction, and activation of apoptosis-related pathways.

Experimental and clinical studies indicate that renal dysfunction contributes to myocardial injury through interconnected mechanisms involving oxidative stress, endothelial dysfunction, inflammation, and microcirculatory disturbances. These processes promote cardiomyocyte hypertrophy, vascular remodeling, stromal expansion, and progressive deterioration of myocardial structure. Quantitative morphometric assessment has become an important tool for evaluating the severity of myocardial remodeling and identifying early structural alterations associated with cardiorenal syndrome. Recent studies have also demonstrated that apoptosis plays an important role in myocardial injury associated with renal disease. Increased expression of apoptosis-related proteins, particularly p53, has been linked to cardiomyocyte loss and deterioration of myocardial architecture under conditions of chronic renal dysfunction (Manoharan et al., 2023). Furthermore, age-related changes may aggravate these pathological processes and increase susceptibility to cardiovascular complications.

Taken together, contemporary studies indicate that renal failure induces significant morphometric and histopathological alterations in myocardial tissue through mechanisms involving oxidative stress, endothelial dysfunction, inflammation, and apoptosis. Nevertheless, despite increasing interest in cardiorenal interactions, limited information is available regarding age-dependent morphometric changes in the myocardium during experimentally induced renal failure.

Although previous studies have described cardiovascular complications associated with renal dysfunction, comprehensive age-dependent morphometric evaluation of myocardial remodeling in cisplatin-induced renal failure remains limited. Furthermore, the relationship between structural myocardial alterations and apoptosis-related cellular responses has not been sufficiently characterized across different age groups. Therefore, the novelty of the present study lies in the integrated assessment of morphometric, histopathological, and immunohistochemical changes in the myocardium of rats with experimentally induced renal failure. By combining quantitative morphometric measurements with histological and p53 immunohistochemical analyses, this study provides new evidence regarding age-related patterns of myocardial remodeling and apoptosis in the setting of cardiorenal injury.

Materials and Methods

Animal Allocation, Randomization, and Experimental Design

A total of 243 outbred white rats of both sexes were included in the study. Animals were stratified according to age (3, 6, 9, and 12 months) and then randomly assigned to experimental groups using a simple randomization procedure. The control group consisted of 80 animals, while 163 animals were

allocated to the experimental group.
Within each age category, animals were distributed proportionally to ensure adequate representation for morphometric, histopathological, and immunohistochemical analyses. All animals underwent baseline clinical assessment before inclusion in the experiment.
The study was performed according to a predefined experimental timeline. Following acclimatization and initial allocation, pathological changes were induced as described below. Animals were subsequently subjected to cisplatin administration to induce renal failure and were monitored throughout the experimental period for clinical condition, body weight, food intake, and behavioral changes.
At the end of the observation period, animals were euthanized under anesthesia, and cardiac tissues were collected for morphometric, histological, and immunohistochemical investigations. All tissue analyses were performed according to identical protocols to minimize methodological variability between age groups.

***Initially, animals were divided into two groups*:**
Control group (n = 80): intact animals maintained under standard laboratory conditions.
Experimental group (n = 163): animals subjected to induction of experimental renal failure by cisplatin administration.
Experimental renal failure was induced by intravenous administration of cisplatin at a dose of 0.5 mg/kg body weight. Following cisplatin administration, animals were monitored daily for behavioral changes, body weight, food intake, and general physiological status throughout the observation period.
Animals demonstrating pathological changes were subsequently subjected to induction of renal injury.
Experimental renal failure was induced by intravenous administration of cisplatin at a dose of 0.5 mg/kg body weight. Following cisplatin administration, animals were monitored daily for behavioral changes, body weight, food intake, and general physiological status.
At the completion of the experimental period, animals were euthanized under appropriate anesthesia, and heart tissues were harvested for morphometric and histopathological examination.
Cardiac morphometric evaluation included determination of:
Body weight (g);
Absolute heart weight (mg);
Relative heart weight index;
Heart length (cm);
Thickness of the endocardium, myocardium, and epicardium (mm);
Cardiomyocyte diameter (μm);
Cardiomyocyte length (μm);
Cardiomyocyte nuclear diameter (μm);
Cardiomyocyte cross-sectional area (μm²);
Diameter of myocardial blood vessels (μm);
Vascular lumen diameter (μm);
Stromal connective tissue thickness (μm).
Measurements were performed using digital microscopy and image analysis software calibrated for morphometric investigations.
Heart tissue samples were fixed in 10% neutral buffered formalin, dehydrated through graded ethanol solutions, cleared in xylene, and embedded in paraffin blocks. Sections 5–7 μm thick were prepared using a semi-automatic rotary microtome and mounted on glass slides.
Histological sections were stained with:
Hematoxylin and eosin (H&E) for general tissue architecture;
Van Gieson stain for assessment of connective tissue and collagen fibers.
Microscopic examination was performed using a light microscope equipped with a digital imaging system. Particular attention was paid to vascular alterations, cardiomyocyte morphology, stromal remodeling, inflammatory infiltration, and degenerative changes.
All photomicrographs were acquired under identical imaging conditions. Scale bars were added using calibrated image-analysis software to ensure accurate representation of tissue dimensions.
Immunohistochemical assessment of myocardial tissue included evaluation of p53 protein expression. Tissue sections were processed according to standard immunohistochemical protocols. Positive and negative cells were counted in representative microscopic fields, and the percentage of positive expression was calculated.
Statistical analysis was performed using IBM SPSS Statistics software (Version 26.0; IBM Corp.,

Armonk, NY, USA). Quantitative data were expressed as mean ± standard error of the mean (Mean ± SEM).

Prior to comparative analyses, data distribution was assessed using the Shapiro–Wilk normality test. Variables demonstrating normal distribution were analyzed using parametric statistical methods.

Comparisons between two groups were performed using Student's t-test, while comparisons among multiple age groups were conducted using one-way analysis of variance (ANOVA). When ANOVA revealed significant differences, Tukey's post-hoc multiple comparison test was applied to identify intergroup differences.

Exact p-values were calculated whenever possible and are reported throughout the Results section. Statistical significance was accepted at $p < 0.05$.

Results, Performance Evaluation, and Discussion

Morphometric analysis demonstrated that experimental renal failure induced significant structural alterations in the myocardium of laboratory rats. Progressive changes were observed in cardiac weight parameters, myocardial wall thickness, cardiomyocyte dimensions, and vascular architecture.

In the experimental group of 3-month-old rats, body weight ranged from 116.25 to 130.48 g, with a mean value of 124.09 ± 0.62 g. Absolute heart weight varied from 461.27 to 576.03 mg, averaging 468.82 ± 5.05 mg. Relative heart weight index averaged 5.12 ± 0.05 mg/g, while heart length reached 0.69 ± 0.04 cm.

Morphometric assessment of the left ventricular wall revealed significant thickening of all cardiac layers in experimental animals compared with age-matched controls. Endocardial thickness increased to 0.26 ± 0.02 mm, myocardial thickness reached 0.91 ± 0.05 mm, and epicardial thickness measured 0.18 ± 0.03 mm. These parameters were significantly higher than those observed in the corresponding control group ($p < 0.05$), indicating early myocardial remodeling associated with cisplatin-induced renal failure.

Cardiomyocyte morphometry demonstrated marked enlargement of myocardial fibers compared with control animals. The mean cardiomyocyte diameter reached 8.05 ± 0.08 μm, while cardiomyocyte length increased to 65.47 ± 2.19 μm. Cardiomyocyte cross-sectional area averaged 483.27 ± 6.73 μm², and nuclear diameter increased to 4.38 ± 0.05 μm. These findings indicate cardiomyocyte hypertrophy and adaptive structural remodeling in response to renal injury.

Analysis of myocardial microvasculature demonstrated significant vascular remodeling compared with control animals, characterized by increased vessel wall thickness and reduced luminal diameter. The average vascular diameter measured 14.52 ± 0.10 μm, whereas the vascular lumen diameter decreased to 6.23 ± 0.05 μm. Stromal connective tissue thickness increased significantly and reached 2.18 ± 0.03 μm (Table 1), reflecting progressive interstitial remodeling of myocardial tissue.

Age-related progression of morphometric alterations was observed in 6-, 9-, and 12-month-old animals. Compared with their respective age-matched control groups, older experimental animals demonstrated more pronounced myocardial remodeling, including progressive cardiomyocyte hypertrophy, increased stromal expansion, and more severe vascular alterations.

Table 1. Age-Dependent Changes in Heart Parameters of Experimental Rats

Parameters	3 months	6 months	9 months	12 months
Body weight (g)	124.09 ± 0.62	183.74 ± 4.43	208.73 ± 5.26	254.83 ± 8.06
Absolute heart weight (mg)	468.82 ± 5.05	629.79 ± 5.36	712.05 ± 5.09	1000.05 ± 9.17
Relative heart weight index (mg/g)	5.12 ± 0.05	4.04 ± 0.05	4.63 ± 0.05	4.76 ± 0.09
Heart length (cm)	0.69 ± 0.04	0.73 ± 0.02	0.85 ± 0.04	1.13 ± 0.04
Endocardial thickness (mm)	0.26 ± 0.02	0.37 ± 0.03	0.36 ± 0.02	0.41 ± 0.03
Myocardial thickness (mm)	0.91 ± 0.05	1.24 ± 0.05	1.59 ± 0.06	2.07 ± 0.05
Epicardial thickness (mm)	0.18 ± 0.03	0.28 ± 0.01	0.30 ± 0.05	0.38 ± 0.04
Cardiomyocyte diameter (μm)	8.05 ± 0.08	8.28 ± 0.37	8.34 ± 0.09	9.10 ± 0.08
Cardiomyocyte length (μm)	65.47 ± 2.19	69.82 ± 4.16	72.68 ± 3.18	73.06 ± 4.65
Cardiomyocyte area (μm²)	483.27 ± 6.73	491.67 ± 5.83	506.71 ± 9.24	522.81 ± 9.16
Number of cardiomyocytes	21.07 ± 0.59	23.28 ± 2.04	23.89 ± 1.47	20.96 ± 1.05

Cardiomyocyte nuclear diameter (μm)	4.38 ± 0.05	4.85 ± 0.08	5.26 ± 0.41	5.32 ± 0.09
Blood vessel diameter (μm)	14.52 ± 0.10	15.27 ± 0.26	15.92 ± 0.31	17.68 ± 1.92
Vascular lumen diameter (μm)	6.23 ± 0.05	6.69 ± 0.05	7.03 ± 0.05	7.59 ± 0.05
Myocardial stromal thickness (μm)	2.18 ± 0.03	2.24 ± 0.04	2.29 ± 0.03	3.15 ± 0.03

Values are expressed as mean ± SEM.
*$p < 0.05$ versus age-matched control group, ** $p < 0.01$ versus age-matched control group, *** $p < 0.001$ versus age-matched control group.*

Across all age categories, morphometric parameters of the myocardium were consistently higher in experimental animals than in age-matched controls, supporting the progressive nature of myocardial remodeling induced by cisplatin-associated renal failure.
Histological examination of myocardial tissue in control animals revealed normal cardiac architecture characterized by regularly arranged cardiomyocyte bundles, intact vascular structures, and minimal connective tissue between muscle fibers.
In contrast, myocardial tissue obtained from rats with experimental renal failure exhibited substantial pathological alterations. The most prominent findings included vascular congestion, endothelial dysfunction, interstitial edema, inflammatory cell infiltration, and degenerative changes in cardiomyocytes.

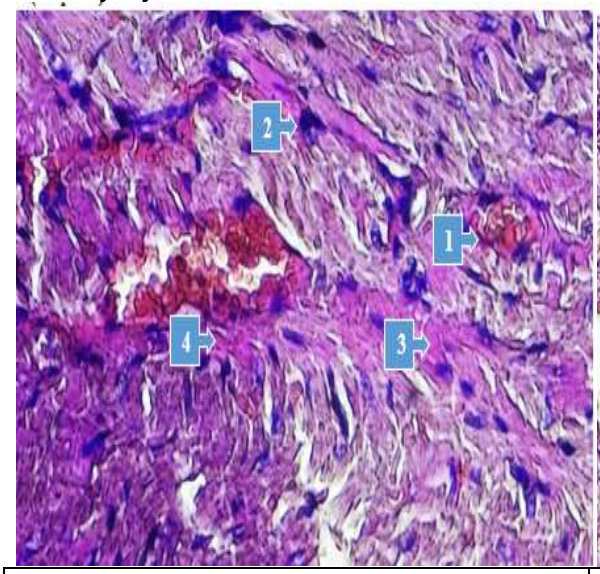

Figure 1. Histological section of the left ventricular myocardium of a 3-month-old rat with cisplatin-induced renal failure. Hematoxylin and eosin staining. Scale bar = 50 μm.

1 – myocardial blood vessel;
2 – cardiomyocyte nucleus;
3 – cardiomyocyte bundle;
4 – thickened vascular wall associated with edema and luminal narrowing.

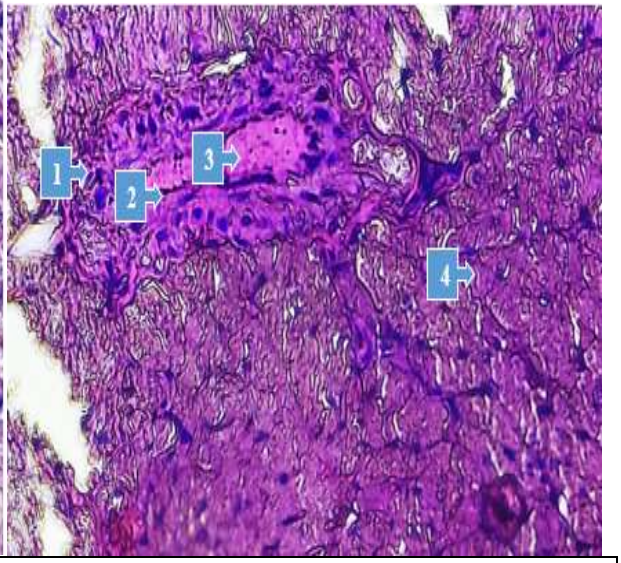

Figure 2. Histological section of the left ventricular myocardium of a 6-month-old rat with cisplatin-induced renal failure. Hematoxylin and eosin staining. Scale bar = 50 μm.

1 – myocardial blood vessel;
2 – vascular endothelial lining;
3 – vascular lumen;
4 – transverse section of cardiomyocytes.

Microscopic examination demonstrated narrowing of vascular lumens associated with endothelial swelling and thickening of vascular walls. Numerous congested vessels containing aggregated erythrocytes were observed throughout the myocardium. Perivascular edema and focal hemorrhagic areas were also detected.

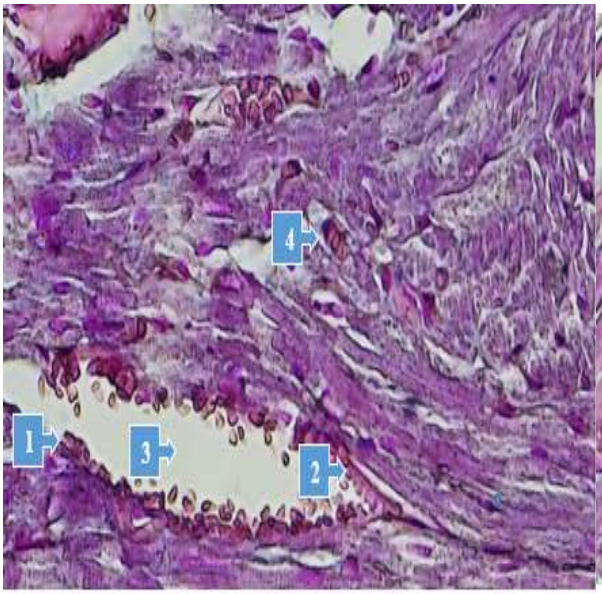

Figure 3. Histological section of the left ventricular myocardium of a 9-month-old rat with cisplatin-induced renal failure. Hematoxylin and eosin staining. Scale bar = 50 µm.
1 – myocardial blood vessel;
2 – vascular endothelial lining;
3 – vascular lumen;
4 – extravasated erythrocytes within the myocardial interstitium.

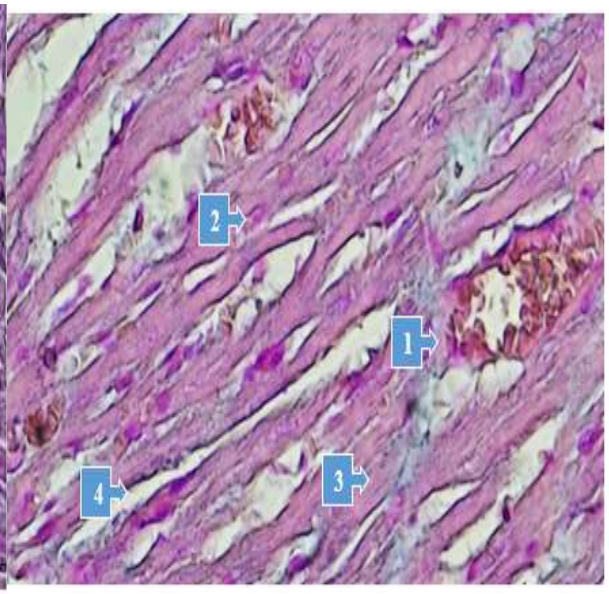

Figure 4. Histological section of the left ventricular myocardium of a 12-month-old rat with cisplatin-induced renal failure. Hematoxylin and eosin staining. Scale bar = 50 µm.
1 – congested myocardial blood vessel;
2 – cardiomyocyte nucleus;
3 – cardiomyocyte bundle;
4 – myocardial stromal thickening.

Degenerative alterations in cardiomyocytes included cytoplasmic swelling, loss of normal cellular organization, nuclear pyknosis, karyolysis, and focal cytolytic changes. In several specimens, diffuse inflammatory infiltration composed predominantly of neutrophils and eosinophilic granulocytes was identified within the myocardial interstitium.

Immunohistochemical analysis demonstrated positive p53 expression in damaged myocardial cells. A total of 294 cells were analyzed, of which 111 cells exhibited positive immunoreactivity, corresponding to an overall expression rate of 37.75%. Positive staining was predominantly localized in areas exhibiting marked cardiomyocyte degeneration and vascular abnormalities, indicating activation of apoptosis-related pathways in response to myocardial injury.

However, no significant association was identified between p53 overexpression and the age of the experimental animals. Likewise, p53 expression did not show a significant correlation with the degree of histological differentiation or the severity of cardiomyocyte injury. These findings suggest that activation of p53-dependent apoptotic pathways may occur independently of age-related factors and primarily reflects cellular responses to myocardial damage induced by experimental renal failure.The increased expression of p53 indicates activation of apoptosis-related pathways in cardiomyocytes under conditions of experimental renal failure. Enhanced apoptotic activity was particularly evident in areas exhibiting pronounced structural damage and vascular abnormalities.

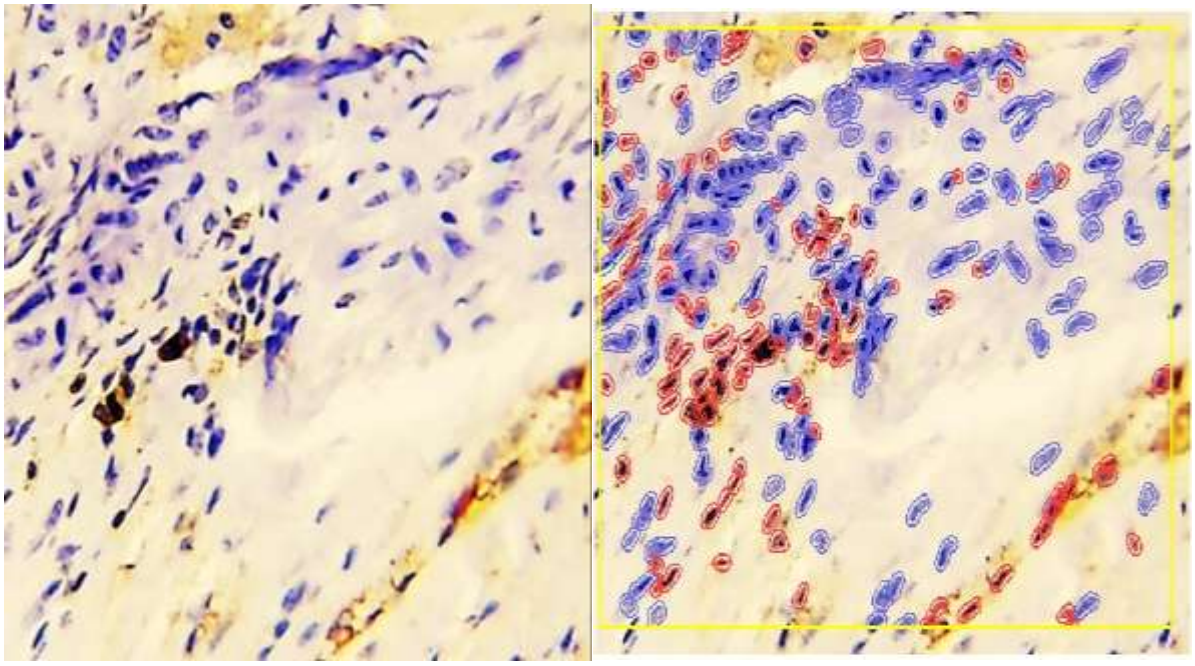

Figure 5. Immunohistochemical staining demonstrating p53 expression in the left ventricular myocardium of a 3-month-old rat with cisplatin-induced renal failure. Positive immunoreactivity is indicated by brown nuclear staining. Scale bar = 50 µm.

Parameter	Value
Total number of analyzed cells	294
Number of positive cells	111
Number of negative cells	183
Positive expression (%)	37.75%
Total area (px^2)	361,472

Overall, the obtained results demonstrate that experimental renal failure is associated with progressive morphometric remodeling, vascular injury, cardiomyocyte degeneration, and activation of apoptosis-related mechanisms in myocardial tissue.

Discussion

The present study demonstrated that experimental renal failure induced significant morphometric and histopathological alterations in myocardial tissue. Structural remodeling was characterized by cardiomyocyte hypertrophy, thickening of myocardial layers, vascular abnormalities, stromal expansion, and increased apoptotic activity. These findings indicate that renal dysfunction exerts substantial adverse effects on cardiac morphology and supports the concept of cardiorenal interaction.

One of the most prominent findings of the present investigation was the increase in cardiomyocyte dimensions accompanied by thickening of the myocardial wall. Similar observations have been reported in previous experimental studies demonstrating that chronic renal dysfunction promotes myocardial hypertrophy through activation of neurohumoral pathways, oxidative stress, and persistent inflammatory responses. Increased cardiomyocyte size is generally regarded as an adaptive response to chronic systemic stress; however, prolonged hypertrophy eventually contributes to myocardial dysfunction and structural deterioration.

The observed vascular alterations, including endothelial injury, luminal narrowing, congestion, and perivascular edema, indicate significant disturbances of myocardial microcirculation. Endothelial dysfunction is considered one of the earliest manifestations of cardiorenal syndrome and plays a critical role in the progression of cardiovascular complications associated with renal disease. Impaired endothelial integrity reduces tissue perfusion, promotes inflammatory activation, and accelerates myocardial remodeling.

Endothelial injury may represent one of the central mechanisms underlying myocardial remodeling in experimental renal failure. Renal dysfunction is associated with increased production of reactive oxygen species and reduced nitric oxide bioavailability, resulting in endothelial activation and impaired

vasodilatory capacity. These changes promote vascular permeability, leukocyte adhesion, microvascular congestion, and tissue hypoxia. Persistent endothelial dysfunction contributes to chronic microcirculatory impairment and accelerates the progression of myocardial structural damage.

Histological examination revealed interstitial inflammatory infiltration and stromal thickening. These findings are consistent with reports indicating that chronic renal injury stimulates systemic inflammatory pathways and excessive extracellular matrix deposition. Persistent inflammation promotes fibroblast activation and collagen accumulation, leading to myocardial fibrosis and impaired cardiac compliance. Increased connective tissue deposition observed in the present study may therefore represent an important mechanism contributing to cardiac remodeling during renal failure.

Another important observation was the presence of degenerative changes in cardiomyocytes, including cytoplasmic swelling, karyolysis, and focal cytolytic alterations. These pathological changes suggest progressive cellular injury caused by metabolic disturbances and oxidative stress. Renal insufficiency is known to increase the accumulation of reactive oxygen species, resulting in lipid peroxidation, mitochondrial dysfunction, and DNA damage. Such mechanisms have been identified as major contributors to myocardial degeneration in both experimental and clinical studies.

The present findings are also consistent with recent experimental studies investigating cisplatin-induced cardiotoxicity. Previous reports have demonstrated that cisplatin administration can directly induce myocardial injury through excessive oxidative stress, mitochondrial dysfunction, inflammatory activation, and apoptosis. Histopathological manifestations described in these studies include cardiomyocyte degeneration, vascular congestion, interstitial edema, and myocardial fibrosis, which closely resemble the alterations observed in the current investigation. Moreover, increased expression of apoptosis-related markers, including p53 and caspase-dependent signaling pathways, has been reported in experimental models of cisplatin toxicity. These observations suggest that myocardial injury in the present study may result not only from cardiorenal interactions secondary to renal dysfunction but also from direct cardiotoxic effects of cisplatin, thereby amplifying structural myocardial remodeling.

The observed stromal expansion may also reflect progressive fibrotic remodeling of the myocardium. Oxidative stress and inflammatory mediators are known to stimulate fibroblast proliferation and extracellular matrix deposition through activation of transforming growth factor-beta (TGF-β) and other profibrotic signaling pathways. Excessive collagen accumulation increases myocardial stiffness, disrupts normal tissue architecture, and contributes to deterioration of cardiac function. The increase in stromal connective tissue thickness identified in the present study is consistent with early stages of myocardial fibrosis described in experimental models of renal and cardiovascular disease.

Oxidative stress is considered a key pathogenic link between renal dysfunction and myocardial injury. Excessive generation of reactive oxygen species not only damages cellular membranes and mitochondrial structures but also activates inflammatory and apoptotic signaling pathways. These processes promote cardiomyocyte hypertrophy, cellular degeneration, and progressive myocardial remodeling. The increased p53 expression observed in the present study may partly reflect oxidative stress-induced activation of apoptosis-related mechanisms within damaged cardiomyocytes.

Age-dependent progression of morphometric alterations was also observed. Older animals demonstrated more pronounced structural changes than younger groups. This finding may be associated with reduced regenerative capacity, cumulative oxidative damage, and age-related decline of adaptive mechanisms. Previous investigations have similarly reported that aging enhances susceptibility to both renal and cardiovascular injury.

Collectively, the obtained results support the concept that renal failure induces complex myocardial remodeling involving vascular injury, inflammatory activation, connective tissue proliferation, cardiomyocyte hypertrophy, and apoptosis. These mechanisms are closely interconnected and contribute to the development of structural cardiac abnormalities characteristic of cardiorenal syndrome.

Recent experimental investigations have further emphasized that cisplatin-associated cardiac injury involves multiple overlapping mechanisms, including oxidative damage, endothelial dysfunction, calcium homeostasis disturbances, and activation of pro-inflammatory cytokines. The morphometric and histopathological alterations identified in the present study support these observations and provide additional evidence that myocardial remodeling develops progressively with advancing age under conditions of cisplatin-induced renal injury.

The present study expands current knowledge regarding myocardial alterations associated with experimental renal failure and provides additional morphometric evidence supporting the existence of a strong pathophysiological relationship between kidney dysfunction and cardiovascular remodeling.

Recent investigations have highlighted the growing importance of cardiorenal interactions in cisplatin-associated toxicity. Experimental studies have demonstrated that cisplatin-induced renal injury contributes to secondary cardiovascular alterations through oxidative stress, systemic inflammation, endothelial dysfunction, and activation of profibrotic signaling pathways. These mechanisms promote myocardial remodeling and increase susceptibility to cardiac dysfunction. The present findings are in agreement with these observations and provide additional morphological evidence supporting the role of cardiorenal syndrome in the progression of myocardial injury.

Conclusion

Experimental renal failure resulted in significant morphometric and histopathological alterations in the myocardium of laboratory rats. The most prominent changes included cardiomyocyte hypertrophy, thickening of myocardial layers, vascular remodeling, stromal expansion, inflammatory infiltration, and degenerative cellular alterations.

Histological examination demonstrated endothelial dysfunction, vascular congestion, interstitial edema, and progressive connective tissue proliferation, indicating substantial myocardial remodeling under conditions of renal impairment. Immunohistochemical analysis further revealed increased p53 expression, suggesting activation of apoptosis-related mechanisms in damaged cardiac tissue.

The severity of structural alterations increased with animal age, reflecting progressive deterioration of adaptive and regenerative capacities. These findings confirm the existence of a close relationship between renal dysfunction and myocardial injury and provide experimental evidence supporting the development of cardiorenal syndrome.

The obtained results may contribute to a better understanding of the mechanisms underlying cardiovascular complications in renal disease and may serve as a morphological basis for future studies aimed at preventing and correcting cardiorenal pathology

Author Contributions

All authors contributed equally to this work and approved the final version of the manuscript.

Conflict of Interest

The authors declare no conflict of interest.

References

1. Abdel-Daim, M. M., Aleya, L., & Alkahtani, S. (2024). Oxidative stress and myocardial injury associated with cisplatin toxicity: Current experimental evidence. *Chemico-Biological Interactions, 387*, 110847.

2. Abdel-Daim, M. M., Aleya, L., & Alkahtani, S. (2024). Oxidative stress, apoptosis, and myocardial injury associated with cisplatin toxicity: Experimental evidence and therapeutic perspectives. *Chemico-Biological Interactions, 387*, 110847.

3. Almeer, R. S., & Abdel Moneim, A. E. (2023). Histopathological and molecular mechanisms of cisplatin-induced cardiac damage. *Biomedicine & Pharmacotherapy, 168*, 115728.

4. Ammar, H. I., Sequiera, G. L., Nashed, M. B., et al. (2024). Oxidative stress and myocardial remodeling in experimental renal failure. Antioxidants, 13(2), 187.
https://doi.org/10.3390/antiox13020187

5. Bansal, N., Katz, R., Dalrymple, L., et al. (2023). Kidney function decline and cardiovascular disease progression. Journal of the American Heart Association, 12(9).
https://doi.org/10.1161/JAHA.123.028745

6. Chen, L., Zhao, Y., Liu, X., Wang, T., & Zhang, J. (2024). Myocardial apoptosis and p53 signaling pathway activation during chronic kidney injury. Cell Death Discovery, 10(1), 96.
https://doi.org/10.1038/s41420-024-01896-5

7. El-Awady, E. S., Moustafa, Y. M., Abo-Elmatty, D. M., & Radwan, A. (2024). Cisplatin-induced cardiotoxicity: Mechanisms and cardioprotective strategies. *European Journal of Pharmacology, 972*, 176312.

8. El-Awady, E. S., Moustafa, Y. M., Abo-Elmatty, D. M., & Radwan, A. (2024). Mechanisms of cisplatin-induced cardiotoxicity and potential cardioprotective strategies. *European Journal of Pharmacology, 972*, 176312.

9. He, L., Wei, Q., Liu, J., Yi, M., Liu, Y., & Liu, H. (2024). Mechanisms of cisplatin-induced nephrotoxicity and cardiotoxicity: Oxidative stress and inflammatory pathways. Frontiers in Pharmacology, 15, 1356724. https://doi.org/10.3389/fphar.2024.1356724
10.House, A. A., Wanner, C., Sarnak, M. J., Piña, I. L., McIntyre, C. W., Komenda, P., et al. (2022). Heart failure in chronic kidney disease: Conclusions from a Kidney Disease: Improving Global Outcomes conference. Kidney International, 101(2), 219–231.
https://doi.org/10.1016/j.kint.2021.09.031Ji Y, Chen H, Wang L, et al. Molecular mechanisms of cardiorenal interaction and myocardial injury during renal insufficiency. Int J Cardiol. 2025;410:132456. doi:10.1016/j.ijcard.2025.132456.
11.Khatun, A., Rahman, M., Sultana, S., et al. (2024). Histopathological evaluation of myocardial fibrosis associated with chronic renal injury. *Tissue and Cell, 87*, 102348.
https://doi.org/10.1016/j.tice.2024.102348
12.Kooman, J. P., Kotanko, P., Schols, A. M. W. J., Shiels, P. G., & Stenvinkel, P. (2023). Chronic kidney disease and cardiovascular remodeling: Current concepts and future perspectives. *Nature Reviews Nephrology, 19*(11), 689–705. https://doi.org/10.1038/s41581-023-00728-1
13.Liu, H., Zhang, W., Wang, Y., et al. (2024). Endothelial dysfunction and cardiovascular remodeling in chronic kidney disease. *International Journal of Molecular Sciences, 25*(3), 1458.
https://doi.org/10.3390/ijms25031458
14.Manoharan, S., Prabu, S. M., Shenbagam, M., & Kumar, R. S. (2023). Role of apoptosis and oxidative stress in cardiovascular complications associated with renal dysfunction. *Life Sciences, 329*, 121911. https://doi.org/10.1016/j.lfs.2023.121911
15.McCullough, P. A., & Ahmad, A. (2023). Cardiorenal syndrome: Epidemiology, pathophysiology and treatment. *World Journal of Cardiology, 15*(4), 183–197.
16.Teshayev Sh.J., Qodirov O.O‘., et al. (2026). Morphometric and Histological Alterations in the Spleen Induced by Chronic Carbon Monoxide Exposure and the Corrective Effects of Gulimaxsar. Natural and Engineering Sciences, 10.28978/nesciences.262009
17.Musial, D. C., Tokarz, A., Cisek, R., et al. (2024). Cardiorenal syndrome and cardiovascular remodeling in experimental kidney injury: Recent advances and future perspectives. *Frontiers in Cardiovascular Medicine, 11*, 1354821.
18.Ning, X., Li, Y., Huang, J., Wang, P., & Zhang, H. (2024). Oxidative stress-mediated myocardial injury in experimental nephrotoxicity models. *Antioxidants, 13*(6), 701.
https://doi.org/10.3390/antiox13060701
19.Ozkok, A., & Edelstein, C. L. (2023). Pathophysiology of cisplatin-induced acute kidney injury. *BioMed Research International, 2023*, 8845672. https://doi.org/10.1155/2023/8845672
20.Pabla, N., & Dong, Z. (2022). Cisplatin nephrotoxicity: Mechanisms and renoprotective strategies. *Kidney International, 102*(4), 777–791. https://doi.org/10.1016/j.kint.2022.05.019
21.Rahman, M. M., Hasan, M., Islam, M. R., & Hossain, S. (2025). Morphometric and histological evaluation of myocardial remodeling in experimental kidney disease. *Journal of Morphological Sciences, 42*(1), 15–24.
22.Rangaswami, J., Bhalla, V., Blair, J. E. A., Chang, T. I., Costa, S., Lentine, K. L., et al. (2023). Cardiorenal syndrome: Classification, pathophysiology, diagnosis, and treatment strategies. *Circulation, 147*(8). https://doi.org/10.1161/CIRCULATIONAHA.122.060789
23.Ronco, C., Bellasi, A., & Di Lullo, L. (2023). Cardiorenal syndrome: An overview. *Advances in Chronic Kidney Disease, 30*(1), 1–10. https://doi.org/10.1053/j.ackd.2022.09.001
24.Ronco, C., Bellasi, A., & Di Lullo, L. (2024). Cardiorenal syndrome: Pathophysiological mechanisms linking kidney and heart dysfunction. *Advances in Chronic Kidney Disease, 31*(2), 95–104.
25.Venkataraman, R., & Kellum, J. A. (2022). Cardiorenal interactions and organ cross-talk in kidney disease. *Critical Care Clinics, 38*(2), 279–294. https://doi.org/10.1016/j.ccc.2021.11.007
26.Wang, X., Zhang, Y., Li, H., & Chen, R. (2024). Histopathological and molecular mechanisms of myocardial injury induced by cisplatin treatment in experimental animals. *Biomedicine & Pharmacotherapy, 176*, 116782.
27.Zhang, Y., Wang, X., Li, H., Zhou, Q., & Chen, R. (2024). Histopathological changes in cardiac tissue associated with renal dysfunction: An experimental study. *Histology and Histopathology, 39*(5), 563–575. https://doi.org/10.14670/HH-18-754